

# Areal distribution of the oxygen-isotope ratio in Antarctica: an assessment based on multivariate models

MARIO B. GIOVINETTO,<sup>1</sup> H. JAY ZWALLY<sup>2</sup>

<sup>1</sup>Earth Sciences 356, University of Calgary, Calgary, Alberta T2N 1N4, Canada

<sup>2</sup>Code 971, NASA/Goddard Space Flight Center, Greenbelt, MD 20771, U.S.A.

**ABSTRACT.** Mean oxygen-isotope ratio values relative to standard mean ocean water ( $\delta^{18}\text{O}$ , in ‰) reported for 406 sites in Antarctica are compiled together with data on mean annual surface temperature, latitude, surface elevation, and mean annual shortest distance to open ocean denoted by the 20% sea-ice concentration boundary. Stepwise regression analyses with  $\delta^{18}\text{O}$  as the dependent variable are used as a model-building procedure based on statistical, rather than physical, criteria. Multivariate models sensitive to covariation between independent variables are defined using the whole dataset ( $N=406$  where  $N$  denotes the number of sites), as well as sub-sets for areas of continuous grounded ice ( $N=206$ ) and ice shelf ( $N=110$ ). The models show improvement over bivariate regression models. Distance to the open ocean enters all models at the second step. Inversions of the set and sub-set models applied to a database for 1351 gridpoint locations 100 km apart (it excludes the regions of Graham Land and eastern Palmer Land) are used to produce contoured distributions of  $\delta^{18}\text{O}$ . These may be used to assess the effects of atmospheric advection, as well as derive ice-flow adjustments for  $\delta^{18}\text{O}$  series obtained from deep-core or ablation-zone samples. Suggestions are made to improve model reliability.

## INTRODUCTION

The areal distribution of  $\delta^{18}\text{O}$  (multi-year mean value of  $^{18}\text{O}/^{16}\text{O}$  relative to standard mean ocean water (SMOW), in ‰) in Antarctica has been discussed, among others, by Morgan (1982), Lorius (1983), and Qin and others (1994). In general, most of the studies concentrate on the strong correlation between  $\delta^{18}\text{O}$  and  $T$  (multi-year mean surface temperature, in K), but other variables and parameters are considered (e.g. Fisher and Alt, 1985; Jouzel and others, 1987). This study presents multivariate models in which  $\delta^{18}\text{O}$  is the dependent variable; the independent variables include  $T$ ,  $L$  (latitude in degrees south),  $H$  (surface elevation in m), and  $D$  (multi-year mean shortest distance to open ocean denoted by the 20% sea-ice concentration boundary in km). There is no significant change in the statistics if a different concentration is used (e.g. 10%).

Stepwise regression analysis is used as a model-building procedure that is sensitive to covariation between independent variables (e.g. Cochran, 1957; Davis and Sampson, 1973). At each step the variable that contributes most to increasing  $R^2$  (the coefficient of determination) enters a model on the basis of statistical rather than physical criteria. Inversions of these models are applied to a database for 1351 gridpoint locations 100 km apart to produce distributions of  $\delta^{18}\text{O}$  for grounded-ice and ice-shelf areas.

In the following sections, all statistics are significant at the 99.99% confidence level ( $F$  statistic under the null hypothesis showing a probability  $P \leq 0.0001$ ) unless stated otherwise. The exceptions to this are some listings of  $R$  (correlation coefficient) in correlation matrices as well as  $R_p$  (partial correlation coefficient) entries in the stepwise procedures in which some  $R$ ,  $R_p$  values  $\ll 0.5$  would corres-

pond to  $P \gg 0.0001$ . These ancillary statistics are separate from (i) the confidence level selected to perform a particular analysis and determine which variables contribute at that level (or better) to the explanation of variation, and (ii) the  $P$  value attained by the model (e.g. Tabachnick and Fidell, 1989).

## SAMPLE SITE DATABASE

The location of 443 sites in Antarctica for which  $\delta^{18}\text{O}$  values have been reported are shown in Figure 1. The base map was not corrected following major calving events of the last two decades; otherwise some sites would appear to lie on the ocean. The compilation for this study includes data for 189 sites from 22 sources as listed by Morgan (1982), which includes a site on sea ice, and for another 254 sites as reported by Clausen and others (1979), Aristarain (1980), Lorius (1983), Potter and others (1984), Reinwarth and Graf (1985), Reinwarth and others (1985), Mosley-Thompson (1992), Peel (1992), Graf and others (1994), Isaksson and Karlén (1994), Qin and others (1994) and Ren and others (1995). Of these, data for 33 sites in Graham Land and eastern Palmer Land regions (grounded ice, ice shelf and island areas) will be analyzed in a separate study. Notices of  $\delta^{18}\text{O}$  data for a total of approximately 20 other sites were received after the completion of the analyses (separate personal communications from M. Craven, E. Isaksson, and V. Morgan, August 1996).

Data on three independent variables ( $L$ ,  $H$ ,  $T$ ) were obtained from the original sources for approximately three-quarters of the sites. Missing  $H$  and  $T$  data were obtained by interpolation from maps of surface contour lines (Drewry, 1983) and surface isotherms (Giovinetto and

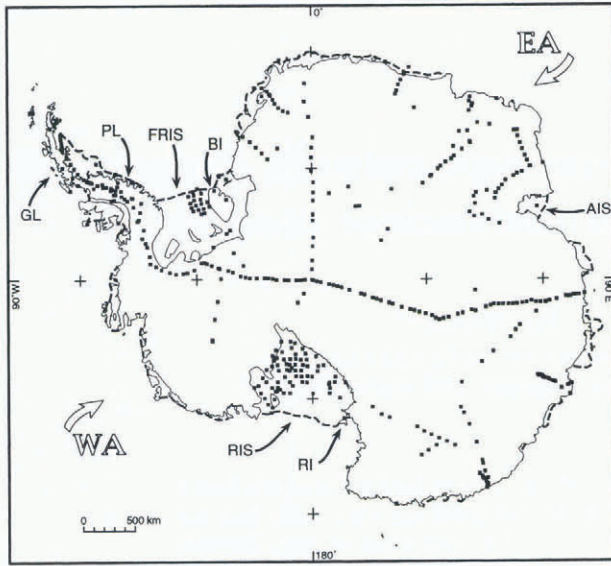


Fig. 1. Antarctica, showing the location of 443 sites for which  $\delta^{18}\text{O}$  values have been reported (full squares). Site locations are correct relative to coordinates; the base map in plotting software is not up to date. Named in the text: EA, WA (East and West Antarctica), GL, PL (Graham and Palmer lands), FRIS, AIS, RIS (Filchner–Ronne, Amery, and Ross Ice Shelves), and BI, RI (Berkner and Ross Islands).

others, 1990). Missing  $T$  and/or  $H$  data for four sites could not be reliably obtained by interpolation and were removed from the database. The  $\delta^{18}\text{O}$ ,  $L$ ,  $H$ , and  $T$  data thus assembled in a dataset called  $N406$ ; ( $N$  denotes the number of sites in the set) and were complemented with a determination of  $D$  from a sea-ice distribution compilation (United States Navy, 1985) using a method described in an earlier study (Giovinetto and Zwally, 1996).

Two aspects of the sample site database should be noted. The first is that no attempt was made to reconcile discrepancies in the spatial location of approximately 20 sites sampled by two or more parties at different times. Thus, a site may appear as two or more in Figure 1, and/or may be entered in the database with two or more different values of a particular variable.

The second aspect is that  $\delta^{18}\text{O}$  values for many sites were obtained by conversion of  $\delta D$  ( $^2\text{H}/^1\text{H}$  relative to SMOW in ‰). In the compilation of Morgan (1982), the  $\delta^{18}\text{O}$  values for 35 sites as reported by Lorius and others (1969) were obtained using

$$\delta^{18}\text{O} = (\delta D - 11)/8.1 \quad (1)$$

The  $\delta D$  values reported by Mosley-Thompson (1992) for the South Pole, and Graf and others (1994) for 28 sites on the Filchner–Ronne Ice Shelf, are compiled for this study using

$$\delta^{18}\text{O} = 0.138 + 0.128\delta D \quad (2)$$

which in the format of Equation (1) converts to

$$\delta^{18}\text{O} = (\delta D - 1)/7.8 \quad (3)$$

derived by us from  $\delta^{18}\text{O}$ ,  $\delta D$  data for 103 of 104 sites as reported in Qin and others (1994) ( $R=0.999$  and the root mean square (rms) residual is 2.58).

## GRIDPOINT DATABASE

The origin lines to determine the 1351 gridpoint locations

are meridians  $0^\circ$ – $180^\circ$ , and  $90^\circ\text{W}$ – $90^\circ\text{E}$ . The perimeter of the grid was determined using an updated map (Drewry, 1983), uncorrected for major calving events as stated for Figure 1. The data for each location were obtained by interpolation:  $L_i$  (latitude in degrees south) from a polar stereographic projection with standard parallel at  $71^\circ\text{S}$ ,  $H_i$  (surface elevation in m) from the compilation of Drewry (1983),  $T_i$  (multi-year mean surface temperature in K) from the compilation of Giovinetto and others (1990), and  $D_i$  (multi-year mean shortest distance to the open ocean denoted by the 20% sea-ice concentration boundary in km) obtained from the same source and by the same method as described above for  $D$  in the sample site database.

There is a strong correlation between  $H_i$  and the surface elevation obtained for 1072 of the 1351 gridpoint locations that lie in areas of ERS-1 radar altimeter coverage ( $R$  is 0.985; rms is 203). The large scatter indicates a large error in the  $H_i$  data, which is in part due to round-off (to  $0.1^\circ$ )  $L_i$  and longitude values entered in the database. This implies potential errors in location by several km north to south, and in most areas of at least 1 km east to west, whereas the ERS-1 data resolution is 500 m (Wingham, 1995). Moreover, the rms is largely determined by the disparity noted in approximately 80 gridpoint locations that lie in regions of steep-surface gradient near mountain ranges, ice termini or grounding lines. In these regions, visual interpolation from contour lines to obtain  $H_i$  is not as reliable as in the interior, and the bilinear interpolation from the ERS-1 database may be biased by inclusion of ice shelf or exposed rock areas (satellite altimeters “illuminate” areas with a radius of approximately 10 km (Wingham, 1995)). Substituting satellite altimetry data for those locations improved the correlation between  $H_i$  and ERS-1 data ( $R$  is 0.995; rms is 116). The bulk of the  $H_i$  data are not updated for this study.

There is also a strong correlation and large scatter ( $R$  is 0.978; rms is 2.3) between  $T_i$  and mean annual surface temperature obtained by bilinear interpolation for all gridpoint locations from Nimbus-7 Temperature Humidity Infrared Radiometer (THIR) data for 1979 (Comiso, 1994). The largest discrepancies between the two temperature sets are found, as discussed above in reference to elevation data, in regions of steep-surface gradient. In these regions, the visual interpolation from isotherms to obtain  $T_i$  is not as reliable as in the interior, and the bilinear interpolation from the THIR database with a resolution of about  $30 \times 30$  km (Comiso, 1994) may be biased by inclusion of ice shelf, sea ice, or exposed rock areas. However, no part of the  $T_i$  data were updated for this study because the point-data, on which the isotherms pattern is based, are mostly means for periods of diverse duration lapsing a few decades (Giovinetto and others, 1990), whereas the THIR data are the mean for a single year. Preliminary studies indicate that use of THIR data to derive  $\delta^{18}\text{O}$  would not produce large differences in most of the area of the ice sheet, but could be large ( $\pm 4\%$ ) in parts of some drainage basins.

## ANALYSES

### Sample site dataset (N406)

The descriptive statistics for the sample site dataset are summarized in Table 1, and the correlation matrix is shown in Table 2. As expected, there is a strong correlation between  $\delta^{18}\text{O}$  and  $T$  ( $R$  is 0.959); the mean value of  $R$  for the four

Table 1. Descriptive statistics

Entity	Datasets*		$\delta^{18}\text{O}$	<i>L</i>	<i>H</i>	<i>T</i>	<i>D</i>
	<i>N</i>	Statistic	‰	°S	m	K	km
Ice sheet	406	Mean:	-34.00	76.28	1466	241.2	1251
		Std dev.:	10.70	6.11	1190	12.0	449
Grounded ice	296	Mean:	-36.56	75.03	1984	238.4	1226
		Std dev.:	11.34	6.39	974	12.9	510
Ice shelves	110	Mean:	-27.11	79.65	72	248.5	1319
		Std dev.:	3.42	3.54	28	4.0	196

\* Excluding Graham Land and eastern Palmer Land (grounded ice, ice shelf and island areas).

Table 2. Correlation matrices

	$\delta^{18}\text{O}$	<i>L</i>	<i>H</i>	<i>T</i>	<i>D</i>
Ice sheet ( <i>N</i> 406)					
$\delta^{18}\text{O}$	1.000	-0.428	-0.836	0.959	-0.678
<i>L</i>	-0.428	1.000	-0.029	0.366	0.885
<i>H</i>	-0.836	-0.029	1.000	-0.838	0.291
<i>T</i>	0.959	-0.366	-0.838	1.000	-0.609
<i>D</i>	-0.678	0.885	0.291	-0.609	1.000
Grounded ice ( <i>N</i> 296)					
$\delta^{18}\text{O}$	1.000	-0.642	-0.876	0.959	-0.781
<i>L</i>	-0.642	1.000	0.336	-0.533	0.926
<i>H</i>	-0.876	0.336	1.000	-0.897	0.525
<i>T</i>	0.959	-0.533	-0.897	1.000	-0.699
<i>D</i>	-0.781	0.926	0.525	-0.699	1.000
Ice shelves ( <i>N</i> 110)					
$\delta^{18}\text{O}$	1.000	-0.834	-0.536	0.747	-0.770
<i>L</i>	-0.834	1.000	0.628	-0.770	0.782
<i>H</i>	-0.536	0.628	1.000	-0.607	0.577
<i>T</i>	0.747	-0.770	-0.607	1.000	-0.635
<i>D</i>	-0.770	0.782	0.577	-0.635	1.000

primary regressions (i.e. between  $\delta^{18}\text{O}$  and each of the four independent variables) is 0.725. The covariation between any two independent variables is, at best, moderate. However, the mean *R* value for  $T = f(L)$ ,  $T = f(H)$ , and  $D = f(L)$ ,  $D = f(T)$  is 0.675, (i.e. only 0.050 smaller than the mean for the primary regressions). The lack of correlation between *T* and *L* (*R* is 0.366) should be expected because approximately one-quarter of the data correspond to sites on the Ross and Filchner–Ronne Ice Shelves, where temperature is relatively high in low elevation areas that lie at high latitude. The expected correlation between *T* and *L* is found in the analyses of sub-sets discussed later.

Stepwise analysis of  $\delta^{18}\text{O} = f(L, H, T, D)$  show that all variables enter the model, with *T*, *D*, and *H* contributing noticeable improvements in correlation; *L* enters last contributing a negligible improvement in rms (Table 3). The robust model (*R* is 0.976; rms is 2.33)

$$\delta^{18}\text{O} = -130.762 + 0.484T + (-4.318E - 3D) + (-2.951E - 3H) + (-0.135L) \quad (3)$$

is applied to the grid database to produce the distribution of  $\delta^{18}\text{O}$  shown in Figure 2. This distribution shows general agreement with the range of values and pattern of isopleths drawn by Morgan (1982) in increments of 10‰. The agreement on the range of values falters toward the barrier on the Filchner–Ronne and Ross Ice Shelves. The agreement in pattern is better on East Antarctica than on West Antarctica. The larger dataset and multivariate approach used in

this study supports a more detailed pattern. Nevertheless, it should be noted that the contour increment in Figure 2 (2‰) is smaller than the error of prediction.

### Grounded ice sub-set (*N*296)

The descriptive statistics and correlation matrix for the data obtained from sites that lie on the conterminous grounded ice sheet are listed in Tables 1 and 2. There are strong correlations between  $\delta^{18}\text{O}$  and *T*, and between  $\delta^{18}\text{O}$  and *H* (*R* values of 0.959 and 0.876, respectively). The mean value of *R* for the four primary regressions is 0.815. Covariation between independent variables is strong in the cases of *D* and *L*, and *T* and *H* (*R* values of 0.926 and 0.897, respectively); the mean *R* value for  $T = f(L)$ ,  $T = f(H)$  and  $D = f(L)$ ,  $D = f(T)$  is 0.764 i.e. only 0.051 smaller than the mean for the primary regressions). In this sub-set, covariation between *L* and the other independent variables renders its contribution as not significant.

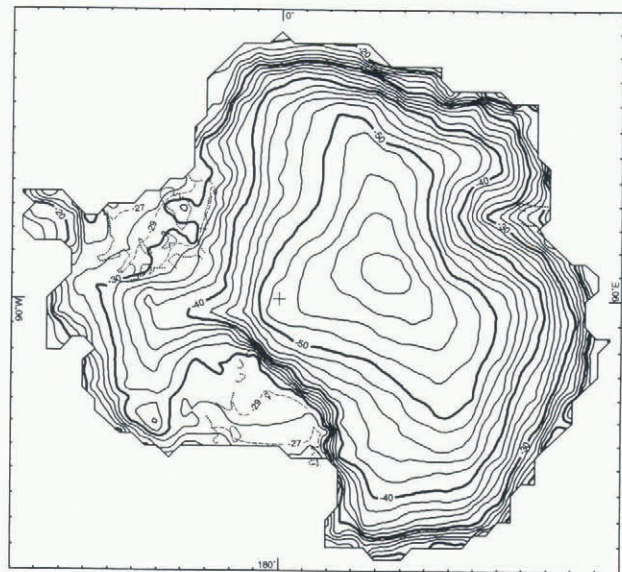


Fig. 2. Distribution of  $\delta^{18}\text{O} = f(T_i, D_i, H_i, L_i)$ . Model based on *N*406 dataset applied to database for 1351 gridpoint locations 100 km apart. Graham Land and eastern Palmer Land regions are omitted. Dotted lines depict grounding lines (the grounding line on the western boundary of the Ross Ice Shelf is roughly coincident with the -30 isopleth). Dashed lines show  $\delta^{18}\text{O}$  contours in increments of 1‰. Ross Island and the northern zone of the Ross Ice Shelf are excluded by the coarse-grid sampling method (the map boundary lies 10 km beyond outer gridpoints).

Stepwise analysis show that only three variables enter the model (*T*, *D*, *H*, in this order; see Table 3); *L* would enter at the 90% confidence level contributing negligible improvements (of the order of  $10^{-4}$ ) in *R* and rms values. The robust model (*R* is 0.976; rms is 2.49)

$$\delta^{18}O = -148.036 + 0.518T + (-5.735E - 3D) + (-2.477E - 3H) \tag{4}$$

is applied to the *N1351* database to produce the distribution of  $\delta^{18}O$  for the grounded ice sheet shown in Figure 3. It is similar to the distribution obtained using Equation (3), except for smoother contours close to the grounding lines, particularly south of the Filchner–Ronne Ice Shelf and east of the Ross Ice Shelf.

**Ice-shelves sub-set (*N110*)**

The descriptive statistics and correlation matrix for the data obtained from sites on ice-shelf areas (including ice rises and islands connected by ice) are also listed in Tables 1 and 2. There is a moderate correlation between  $\delta^{18}O$  and *L* (*R* is 0.834); it is the largest *R* value in the matrix, as well as the largest obtained for the relationship in either the *N406* set or the *N296* sub-set. The mean value of *R* for the three primary regressions (excluding  $\delta^{18}O = f(H)$ ) is 0.784. The mean value of *R* for *T* = *f*(*L*), and *D* = *f*(*L*), *D* = *f*(*T*) is 0.729 (i.e. 0.055 smaller than the mean for the primary regressions). In this sub-set, covariation between *H* and the other independent variables, as well as a weak correlation with  $\delta^{18}O$ , renders its contribution as not significant.

The stepwise analysis shows that only three variables enter the model (*L*, *D* and *T*, in this order; see Table 3); *H* would not enter the model even if run at the 90% confidence level. The robust model (*R* is 0.868, rms is 1.72)

$$\delta^{18}O = -37.581 + (-0.417L) + (-4.951E - 3D) + 0.202T \tag{5}$$

is applied to the *N1351* database to produce the distribution of  $\delta^{18}O$  shown in the area of the Filchner–Ronne and Ross Ice Shelves (Fig. 3). Only a few gridpoints lie on the Amery Ice Shelf; a smaller grid mesh (e.g. 25 km) would be required to produce reliable contours on this, and smaller, ice shelves.

The isopleth values on the Filchner–Ronne and Ross Ice Shelves obtained using Equation (3) show approximately

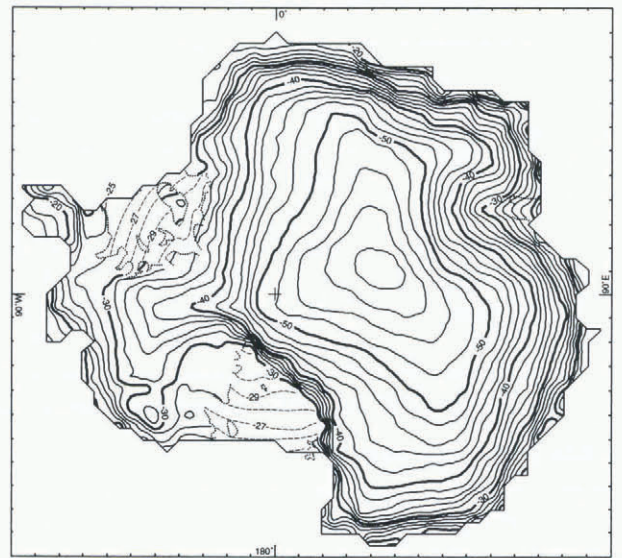


Fig. 3. Distribution of  $\delta^{18}O = f(T_i, D_i, H_i)$  on the continuous grounded ice area based on the *N296* data sub-set, and of  $\delta^{18}O = f(L_i, D_i, T_i)$  on the Filchner–Ronne and Ross Ice Shelves based on the *N110* data sub-set (dashed lines in contour increments of 1‰). Contours on smaller ice shelves are not valid. Produced from the same grid database used for Figure 2.

the same range as those that would be obtained using Equations (4) or (5), except in relatively small regions in the northwest of the Filchner–Ronne Ice Shelf and in the northeast of the Ross Ice Shelf. In most of the area of each ice shelf, the largest difference in  $\delta^{18}O$  values obtained for any gridpoint location using any two models is smaller than the summation of the two smallest predictive errors (square root of the sum of  $rms^2$  is 2.90). Differences in  $\delta^{18}O$  values >2.9‰ are noted between isopleths on the northwestern areas of both ice shelves and isopleths on the grounded ice because of contouring procedures. The general orientation of the isopleths produced by the three models is approximately the same; in the case of Equations (3) and (4) in response to the dominance of the temperature and distance terms, and in the case of Equation (5), due to the strength of the covariation between latitude, temperature, and distance, described above.

Table 3. Summary of stepwise regression analyses ( $\delta^{18}O$  as the dependent variable)

Dataset/stepforward	Independent variable		<i>R</i> (mod.)	Partial correlation coefficient ( <i>R<sub>p</sub></i> )				<i>rms</i> (mod.)
	Inc.	Exc.		<i>L</i>	<i>H</i>	<i>T</i>	<i>D</i>	
<i>N406</i>	/0	—	—	-0.428	-0.836	0.959	-0.678	10.70
	/1	<i>T</i>	0.959	-0.292	-0.207		-0.414	3.04
	/2	<i>T, D</i>	0.966	0.199	-0.532			2.77
	/3	<i>T, D, H</i>	0.976	-0.122				2.35
	/4	<i>T, D, H, L</i>	0.976					2.33
<i>N296</i>	/0	—	—	-0.642	-0.876	0.959	-0.781	11.34
	/1	<i>T</i>	0.960	-0.476	-0.123		-0.547	3.20
	/2	<i>T, D</i>	0.965	0.053	-0.378			2.69
	/3	<i>T, D, H</i>	0.979	0.091				2.49
<i>N110</i>	/0	—	—	-0.834	-0.536	0.747	-0.639	3.42
	/1	<i>L</i>	0.834		-0.029	0.298	-0.447	1.90
	/2	<i>L, D</i>	0.855	0.035	0.288			1.79
	/3	<i>L, D, T</i>	0.868		0.111			1.72

The distribution produced using Equation (5) on the Filchner–Ronne Ice Shelf shows good agreement with the detailed distribution presented by Graf and others (1994) in the area west of Berkner Island, both in  $\delta^{18}\text{O}$  values and in the orientation of the isopleths. However, the distribution on the Ross Ice Shelf shows little agreement with the detailed distribution of  $\delta^{18}\text{O}$  contoured by Clausen and others (1979). There is agreement in the short segments of the  $-31\text{‰}$  and  $-30\text{‰}$  isopleths drawn in the south, and on the isopleth pattern drawn on the northeast, although the modeled  $\delta^{18}\text{O}$  values are isotopically cooler by up to  $\sim 5\text{‰}$  in the small region northeast of Roosevelt Island. The main difference between the two distributions shows in the central and northwestern areas of the ice shelf. There, the isopleths drawn by Clausen and others (1979) show a definite northwest to southeast orientation (rather than the east to west orientation shown in Fig. 3), and the modeled  $\delta^{18}\text{O}$  values are isotopically warmer by up to  $\sim 4\text{‰}$ . It is evident that the modeled distribution in the Ross Ice Shelf has shortcomings which, in part, may be reduced by changes in the contouring algorithm and/or by increasing the grid density (from 100 km to 50 km, thus approaching the sample site “grid” of approximately 55 km used by Clausen and others (1979)). Another possible way to improve the model’s reliability would be to force the stepwise procedure entering temperature first and obtain partial correlations for distance and latitude, to continue the run, or to run these as a set (i.e. use a setwise regression procedure; Tabachnick and Fidell (1989)).

## DISCUSSION AND CONCLUSIONS

In general, inversions of well-documented simple (linear) regression models  $\delta^{18}\text{O} = f(T)$  are used to infer temperature variations from  $\delta^{18}\text{O}$  series obtained in shallow-pit and intermediate-depth ice-core samples. In Table 3 it is shown that such a model, which corresponds to step 1 in the analysis of the *N406* set, is robust:

$$\delta^{18}\text{O} = -239.507 + 0.852 T; \quad (R \text{ is } 0.959; \text{rms is } 3.04) \quad (6)$$

However, adoption of a multivariate model as defined in step 4 of the procedure and described by Equation (3) shows only a minor increase in *R* (0.017) but a significant reduction in rms (0.71). These differences are an assessment of the gain in model reliability attained by the inclusion of distance, elevation and latitude.

The use of stepwise regression analyses to define models and produce contoured areal distributions of  $\delta^{18}\text{O}$  have the attribute of excluding variables that would not add to the explanation of variation. The negative aspect, namely that variables enter a model at particular confidence levels based on statistical rather than physical criteria, should not present a problem if the limitation is clearly understood. Examples of this are found in the analyses of the sub-sets for grounded ice (*N296*) and ice shelves (*N110*):

(i) The analysis of sub-set *N296* shows that after the run  $\delta^{18}\text{O} = f(T)$ , the residual variation of  $\delta^{18}\text{O}$  is best explained by *D* rather than *H*, and second, that *L* does not contribute to the explanation of variation except at the 90% confidence level (and minimally if the procedure is run at that level). The gain in model reliability attained by

the inclusion of *D* and *H* is assessed comparing Equation (4), and the bivariate version

$$\delta^{18}\text{O} = -237.938 + 0.485 T; \quad (R \text{ is } 0.959, \text{rms is } 3.20) \quad (7)$$

It shows a minor increase in *R* (0.023) but a significant reduction in rms (0.71).

(ii) The analysis of sub-set *N110* shows that due to the strength of the covariation between *L*, *D* and *T*, these enter the model in the reverse order than would be suggested on the basis of physical criteria. The relevant aspect is that inversion of Equation (5) produces a more reliable pattern depicting the distribution of  $\delta^{18}\text{O}$  on the basis of temperature alone:

$$\delta^{18}\text{O} = -186.684 + 0.642 T; \quad (R \text{ is } 0.747, \text{rms is } 2.29) \quad (8)$$

The gain in model reliability is assessed by an increase in *R* (0.121) and a reduction in rms (0.57).

The distribution of  $\delta^{18}\text{O}$  produced using Equation (3) (Fig. 2), and that produced using Equation (4) and (5) (Fig. 3), show that the isopleth patterns derived from the sub-sets are less intricate in the zones upwind and downwind from the grounding lines, particularly in the southeastern area of the Filchner–Ronne Ice Shelf. This is a tangible attribute of the combined pattern because the largest differences between  $\delta^{18}\text{O}$  values generated for the ice-shelf areas using Equations (3), (4) or (5) are relatively small, as was discussed in a preceding section.

Caution should be exercised either to define a model using data collected from, or use results of its inversion applied to, locations that lie at  $<100$  km upwind or downwind from grounding lines, or on terminal slopes where the surface gradient is  $>1\%$ . In these zones the proportion of drifting snow mixed with “local” precipitation would be different from a “normal” mix for outlying areas. In the context of this study, inclusion of data from sites to define a model would also affect the reliability of the distributions produced from inversions applied to grid data. The problem can be minimized by removal of data for sites that lie in those zones. To assess this, data for 72 sites that lie in zones as described above were removed from the dataset. Stepwise analysis of the reduced set (*N324*) showed a robust model (*R* is 0.977, rms is 2.22)

$$\delta^{18}\text{O} = -129.565 + 0.504 T + (-3.181 E - 3 D) + (-3.073 E - 3 H) + (-0.226 L) \quad (9)$$

in which the partial correlations were similar through every step; thus, and relative to Equation (3), the variables entered the model in the same order. Nevertheless, there is a reduction in rms of 0.11, and most importantly, changes in the coefficients for *D* and *L* of 26% and 67%, respectively. This suggests that if a much larger number of data sites are compiled in the future, analysis of sub-sets for grounded-ice and ice-shelf areas screened following the criteria described above, could provide improved definitions of Equations (4) and (5), and therefore a more reliable pattern than that shown in Figure 3. The same screening criteria applied to regional datasets (e.g. on the Ross Ice Shelf) showed a relatively greater improvement in *R* and rms values; however, reports for other areas suggest that variations in the proportion of drifting snow do not affect  $\delta^{18}\text{O}$  values (e.g. Bromwich and Weaver, 1983).

The basic models presented (Equations (3), (4) and (5)) show two distributions of  $\delta^{18}\text{O}$  (Figs 2, 3) over a continental-scale area with a relatively large range in latitude, elevation, temperature and distance from source. These are considered in detailed studies of advection (e.g. Robin and Johnsen, 1983; Fisher, 1990) as well as the derivation of ice-flow adjustments for  $\delta^{18}\text{O}$  series obtained from deep ice-core or ablation-zone samples (e.g. Dansgaard and others, 1973; Budd and Young, 1983).

Overall, it should be noted that  $D$  enters all models at the second step, contributing increases in  $R$  values of 0.013 for the grounded-ice model, and of 0.021 for ice-shelf model, as well as decreases in rms of 0.51 and 0.11, respectively. The response of  $\delta^{18}\text{O}$ , as well as  $T$  in the context of  $\delta^{18}\text{O}$  distributions, to distance to open ocean has been noted, among others, by Kato (1979), Koerner (1979), and Bromwich and Weaver (1983). The findings from the stepwise models substantiate those described in the earlier studies based on regional datasets.

## ACKNOWLEDGEMENTS

The authors gratefully acknowledge the contributions of A. J. Aristarain, E. Isaksson, V. I. Morgan, H. Oerter and E. Tull in locating data, of S. Fiegles, S. E. Gammell, D. Phillips, R. E. Poitras, and T. Seiss in data processing, and of V. I. Morgan, E. J. Steig, and N. M. Waters for reviewing the manuscript.

## REFERENCES

- Aristarain, A. J. 1980. *Étude glaciologique de la calotte polaire de l'île James Ross (Péninsule Antarctique)*. Grenoble, CNRS. Laboratoire de Glaciologie et de Géophysique de l'Environnement. (Publ. 322.)
- Bromwich, D. H. and C. J. Weaver. 1983. Latitudinal displacement from main moisture source controls  $\delta^{18}\text{O}$  of snow in coastal Antarctica. *Nature*, **301** (5896), 145–147.
- Budd, W. F. and N. W. Young. 1983. Application of modelling techniques to measured profiles of temperatures and isotopes. In Robin, G. de Q., ed. *The climatic record in polar ice sheets*. Cambridge, etc., Cambridge University Press, 150–177.
- Clausen, H. B., W. Dansgaard, J. O. Nielsen and J. W. Clough. 1979. Surface accumulation on Ross Ice Shelf. *Antarct. J. U.S.*, **14**(5), 68–72.
- Cochran, W. G. 1957. Analysis of covariance: its nature and uses. *Biometrics*, **13**(3), 261–281.
- Comiso, J. C. 1994. Surface temperatures in the polar regions from Nimbus 7 temperature humidity infrared radiometer. *J. Geophys. Res.*, **99**(C3), 5181–5200.
- Dansgaard, W., S. J. Johnsen, H. B. Clausen and N. Gundestrup. 1973. Stable isotope glaciology. *Medd. Grønland*, **197**(2).
- Davis, J. C. and R. J. Sampson. 1973. *Statistics and data analysis in geology. First edition*. New York, etc., John Wiley and Sons.
- Drewry, D. J. 1983. The surface of the Antarctic ice sheet. In Drewry, D. J., ed. *Antarctica: glaciological and geophysical folio*. Cambridge, University of Cambridge. Scott Polar Research Institute, Sheet 2.
- Fisher, D. A. 1990. A zonally-averaged stable-isotope model coupled to a regional variable-elevation stable-isotope model. *Ann. Glaciol.*, **14**, 65–71.
- Fisher, D. A. and B. T. Alt. 1985. A global oxygen isotope model—semi-empirical, zonally averaged. *Ann. Glaciol.*, **7**, 117–124.
- Giovinetto, M. B. and H. J. Zwally. 1996. Annual changes in sea ice extent and of accumulation on ice sheets: implications for sea level variability. *~ Gletscherkd. Glazialgeol.*, **31**, Part 1, 1995, 39–49.
- Giovinetto, M. B., M. N. Waters and C. R. Bentley. 1990. Dependence of Antarctic surface mass balance on temperature, elevation, and distance to open ocean. *J. Geophys. Res.*, **95**(D4), 3517–3531.
- Graf, W. and 6 others. 1994. Snow-accumulation rates and isotopic content ( $^2\text{H}$ ,  $^3\text{H}$ ) of near-surface firn from the Filchner–Ronne Ice Shelf, Antarctica. *Ann. Glaciol.*, **20**, 121–128.
- Isaksson, E. and W. Karlén. 1994. High resolution climatic information from short firn cores, western Dronning Maud Land, Antarctica. *Climatic Change*, **26**(4), 421–434.
- Jouzel, J., G. L. Russell, R. J. Suozzo, R. D. Koster, J. W. C. White and W. S. Broecker. 1987. Simulations of the HDO and  $\text{H}_2^{18}\text{O}$  atmospheric cycles using the NASA GISS general circulation model: the seasonal cycle for present-day conditions. *J. Geophys. Res.*, **92**(D12), 14,739–14,760.
- Kato, K. 1978. Factors controlling oxygen isotopic composition of fallen snow in Antarctica. *Nature*, **272**(5648), 46–48.
- Koerner, R. M. 1979. Accumulation, ablation, and oxygen isotope variations on the Queen Elizabeth Islands ice caps, Canada. *J. Glaciol.*, **22**(86), 25–41.
- Lorius, C. 1983. Antarctica: survey of near-surface mean isotopic values. In Robin, G. de Q., ed. *The climatic record in polar ice sheets*. Cambridge, etc., Cambridge University Press, 52–56.
- Lorius, C., L. Merlivat and R. Hagemann. 1969. Variations in the mean deuterium content of precipitation in Antarctica. *J. Geophys. Res.*, **74**(28), 7027–7031.
- Morgan, V. I. 1982. Antarctic ice sheet surface oxygen isotope values. *J. Glaciol.*, **28**(99), 315–323.
- Mosley-Thompson, E. 1992. Paleoenvironmental conditions in Antarctica since A.D. 1500: ice core evidence. In Bradley, R. S. and P. D. Jones, eds. *Climate since A.D. 1500*. London and New York, Routledge, 572–591.
- Peel, D. A. 1992. Ice core evidence from the Antarctic Peninsula region. In Bradley, R. S. and P. D. Jones, eds. *Climate since A.D. 1500*. London and New York, Routledge, 549–571.
- Potter, J. R., J. G. Paren and J. Loynes. 1984. Glaciological and oceanographic calculations of the mass balance and oxygen isotope ratio of a melting ice shelf. *J. Glaciol.*, **30**(105), 161–170.
- Qin Dahe, J. R. Petit, J. Jouzel and M. Stievenard. 1994. Distribution of stable isotopes in surface snow along the route of the 1990 International Trans-Antarctica Expedition. *J. Glaciol.*, **40**(134), 107–118.
- Reinwarth, O. and W. Graf. 1985. Neuere Untersuchungen zur Akkumulation auf dem Filchner/Ronne-Schelfeis. In Kohnen, H., comp. *Filchner-Ronne-Ice-Shelf Programme. Report 2*. Bremerhaven, Alfred-Wegener-Institute for Polar Research, 7–17.
- Reinwarth, O., W. Graf, W. Stüchler, H. Moser and H. Oerter. 1985. Investigations of the oxygen-18 content of samples from snow pits and ice cores from the Filchner-Ronne Ice Shelves and Ekström Ice Shelf. *Ann. Glaciol.*, **7**, 49–53.
- Ren Jiawen and 8 others. 1995. Glaciological studies on Nelson Island, South Shetland Islands, Antarctica. *J. Glaciol.*, **41**(138), 408–412.
- Robin, G. de Q. and S. J. Johnsen. 1983. Atmospheric processes. In Robin, G. de Q., ed. *The climatic record in polar ice sheets*. Cambridge, etc., Cambridge University Press, 47–52.
- Tabachnick, B. G. and L. S. Fidell. 1989. *Using multivariate statistics. Second edition*. New York, Harper Collins Publishers Inc.
- United States Navy. 1985. *Sea ice climatic atlas. I. Antarctic*. Ashville, NC, U.S. Navy. Naval Oceanography Command Detachment.
- Wingham, D. J. 1995. The limiting resolution of ice-sheet elevations derived from pulse-limited satellite altimetry. *J. Glaciol.*, **41**(138), 413–22.